

CHAPTER 1

INTRODUCTION

1.1 Ferroelectrics

In the half century since Valasek¹ first discovered the ferroelectric effects in Rochlle salt $[\text{NaKC}_4\text{H}_4\text{O}_6 \cdot 4\text{H}_2\text{O}]$, there has been an ever-increasing amount of research and development in these materials. Ferroelectrics are a special class of materials that belongs to the pyroelectric family, of which a permanent electric dipole can be reoriented between equilibrium states by an external electric field. Of the 32 crystallographic point groups, 21 of these are non-centrosymmetric. The 20 non-centrosymmetric classes, excluding (432), are piezoelectric, meaning they exhibit an electric polarization when subjected to a stress. Ten of the 20 piezoelectric classes are polar and develop the charge in polarization with temperature, i.e., pyroelectric. Pyroelectric materials whose polarity can be reversed by application of an electric field are ferroelectric. All ferroelectric materials are, therefore, piezoelectric, but the converse is not true.

As a ferroelectric crystal polarizes, a domain structure is formed. Those domains will initially nucleate randomly with their polarization vectors along one of the symmetry allowed directions. On application of an electric field, polarization switching occurs by the creation and motion of domains. If the field is sufficiently large, the dipole moments of the entire crystal will be aligned. Such a crystal is said to be in the single domain state. The energy required to reorient the domains can then

be seen in the area of electric displacement versus applied field hysteresis loop, as seen in Fig. 1.1.

This loop is usually obtained by applying an alternating voltage with a frequency of less than 60 cycles/sec and measuring the stored charge relative to the instantaneous voltage. The value of P_r , the remanent polarization, is a true measurement of ferroelectricity. This is the polarization that remains once the applied electric field has been removed. It is generally lower for ceramic samples than for single crystal samples because of the increased polycrystalline stress and increased number of domains in ceramics. The energy required to reorient the domains can be estimated from the area of the polarization versus applied field (P/E) hysteresis loop. Ceramic samples exhibit more rounded loops compared to the almost square shaped loop of single crystals. The squareness of the loops obtained from single crystals implies that there is a sudden change in the polarization direction, and generally that there are fewer, and larger, domains compared with ceramic specimens.

The temperature at which the crystal structure transforms from the paraelectric state into the ferroelectric state is called the Curie point.² According to the Curie-Weiss law, the dielectric constant obeys the equation:²

$$\frac{1}{\varepsilon} = \frac{(T - T_0)}{C} \quad (1.1)$$

where, C is the Curie-Weiss constant, T is the temperature and, T_0 is the

Curie-Weiss temperature that is less than T_c . The Curie point is the actual transformation temperature, while the Curie-Weiss temperature is found by

extrapolating the plot of the Curie-Weiss law, as shown in Fig. 1.2. The Curie-Weiss temperature can be as much as ten degrees lower than the Curie point for first-order phase transitions and the two are equal for a second order phase transition. First-order phase transitions are those in which the first derivative of the free energy expansion with respect to temperature is discontinuous. In second-order phase transitions, the second derivate is continuous.

Curie-Weiss law behavior is one of the "tests" for ferroelectricity. Many researchers have used plots like Fig. 1.2 to demonstrate that ferroelectricity is potentially present in a material. While the Curie-Weiss law is a characteristic of ferroelectrics, the ability to re-orient the spontaneous polarization is a necessary condition for ferroelectricity. In summary, when determining whether or not a specimen is a ferroelectric, a number of conditions must be satisfied. The following characteristics can be effective guides: a polar point group, true dielectric hysteresis, a non-zero remanent polarization, and a domain structure that can be reoriented at realistic field levels.

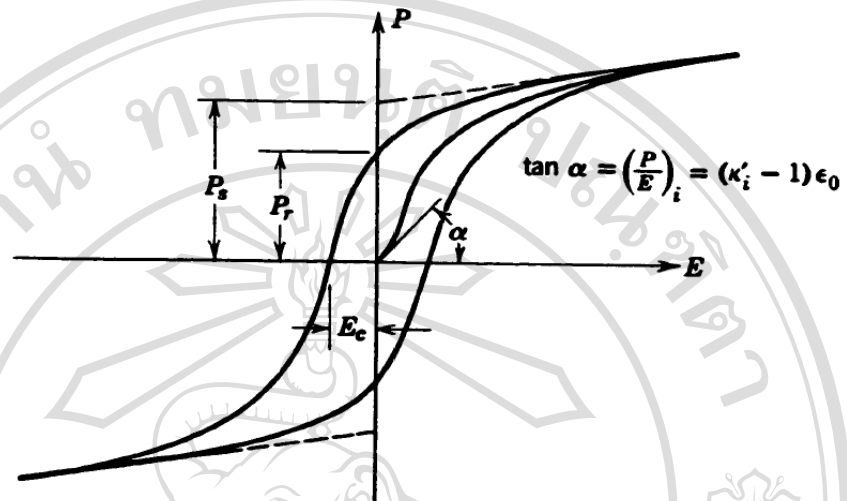


Figure 1.1 A typical ferroelectric hysteresis loop.³

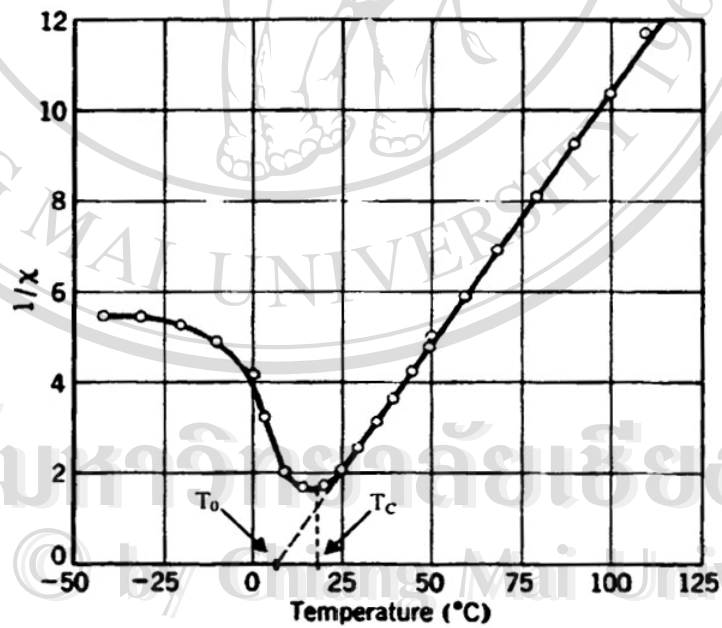


Figure 1.2 Curie-Weiss plot for a barium strontium titanate composition.³

1.2 Relaxor ferroelectrics

1.2.1 Introduction

Relaxor ferroelectrics are a class of materials first synthesized in the 1950's by Smolenskii *et al.*⁴ The materials which called "relaxor" exhibit a broad maximum and a significant frequency dispersion of the dielectric permittivity, with the temperature of the maximal dielectric constant (T_m) increasing and its magnitude ($\epsilon_{r,max}$) decreasing with increasing frequency. The relative permittivity of these materials is also much larger than that of traditional ferroelectric materials, such as BaTiO₃. Relaxor ferroelectric behavior is typically seen in complex perovskites and tungsten bronze families.⁵ Some common examples of relaxor ferroelectrics are Pb(Mg_{1/3}Nb_{2/3})O₃, Pb_{1-x}La_x(Zr_{1-y}Ti_y)_{1-x/4}O₃ (PLZT), and (Pb,Ba)Nb₂O₆ (PBN). There is a wide range of applications for relaxors and relaxor-based solid solutions. These materials have large piezoelectric, electro-optic, dielectric, and pyroelectric properties that can be taken advantage of in the design of new high-performance devices.⁶

1.2.2 Relaxor ferroelectric behavior

The relaxor-ferroelectric behavior of compounds in the complex perovskite family was first reported by Smolenskii *et al.* in the late 1950's.⁴ A general formula for the oxide complex perovskite is:



where the A' and A'' ions are large cations, generally Pb^{2+} , Ba^{2+} , and Sr^{2+} . The B' ion is an ion with a small charge such as Mg^{2+} , Zn^{2+} , Ni^{2+} , and Fe^{2+} . The B'' ion is a highly charged ion such as Nb^{5+} , Ta^{5+} , W^{4+} , or Ti^{4+} . In this class of materials, the initial discovery of relaxor behavior was reported for the compositions, $\text{Pb}(\text{Ni}_{1/3}\text{Nb}_{2/3})\text{O}_3$ [PNN] and $\text{Pb}(\text{Mg}_{1/3}\text{Nb}_{2/3})\text{O}_3$ [PMN]. Since Smolenskii's initial work, relaxor behavior has been observed in a large number of complex perovskites and perovskite-related structures. Some general features of relaxor ferroelectrics have been recognized by Cross⁵, as shown in Table 1.1

The sharp, well-defined phase transition temperature found for normal ferroelectrics is absent in relaxors. The paraelectric to ferroelectric phase transition becomes broad and diffuse in relaxors and a Curie range replaces the Curie temperature. The permittivity of relaxors is also dispersive in nature at radio frequencies, i.e. the permittivity decreases and the temperature at which the permittivity is at maximum, T_{max} , shifts to higher temperatures with increasing frequency.

In relaxor ferroelectrics, the dielectric constant does not follow Curie-Weiss behavior above the ferroelectric transition, but, instead follows the so-called quadratic Curie-Weiss law:^{6,7}

$$\frac{1}{\varepsilon} = \frac{1}{\varepsilon_{\text{max}}} + \frac{(T - T_{\text{max}})^2}{2\delta^2 \varepsilon_{\text{max}}} \quad (1.3)$$

where, ε is the real part of the permittivity, ε_{max} is the permittivity at T_{max} , and δ is the diffuseness parameter. This quadratic relation is valid for materials that display a

diffuse phase transition like the relaxor ferroelectric PMN. Most materials, however, show intermediate behavior between the linear and quadratic limits. Uchino⁸ addressed this by introducing a variable power law:

$$\frac{1}{\varepsilon} = \frac{1}{\varepsilon_{\max}} + \frac{(T - T_{\max})^{\gamma}}{2\delta^{\gamma} \varepsilon_{\max}} \quad (1.4)$$

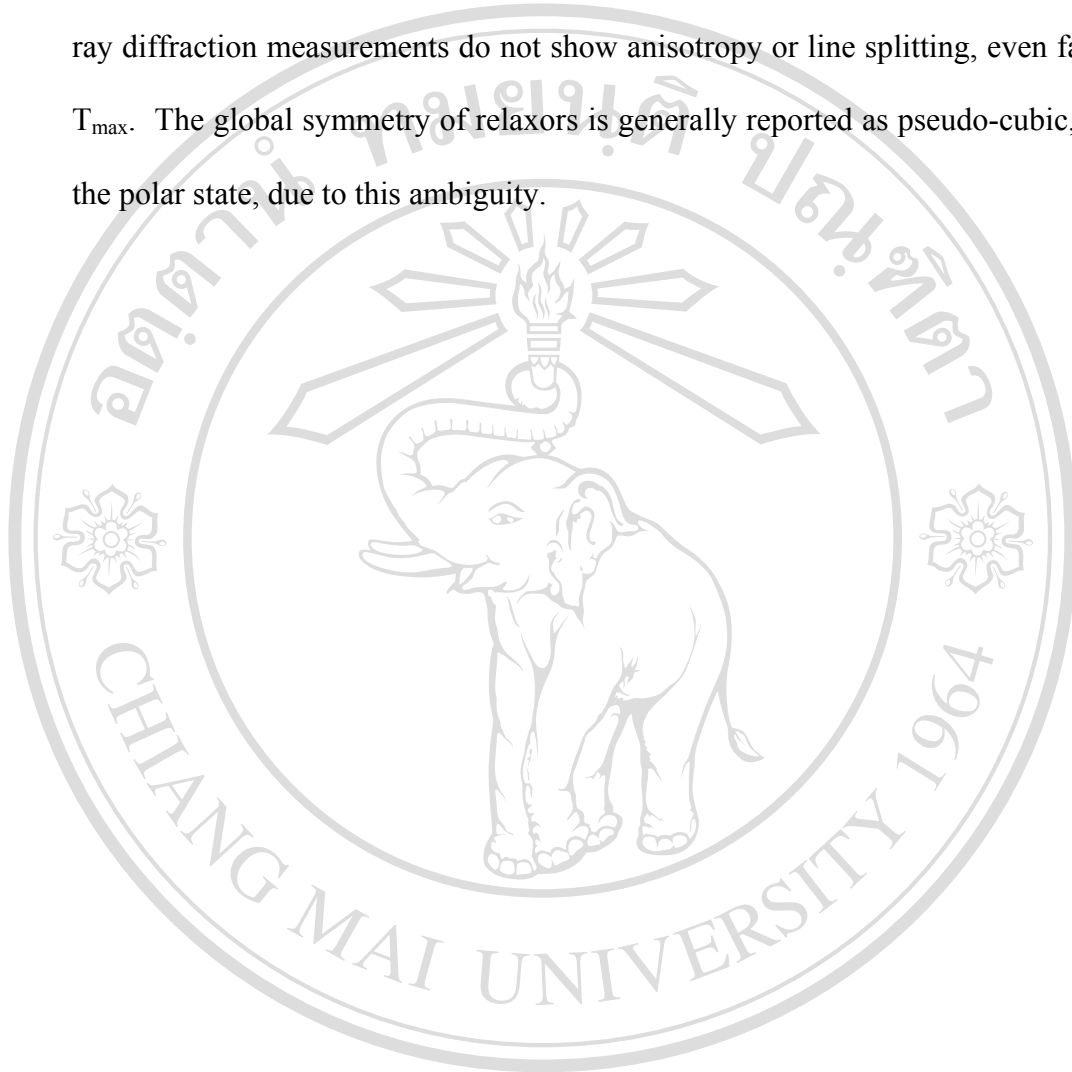
where γ is the critical exponent. The equation (1.3) can be solved graphically using a log-log plot. A slope of this curve represents the value of the critical exponent, γ , and the intercept gives the diffuseness parameter, δ , according to the following equation:

$$\delta = \left(\frac{e^{-\text{intercept}}}{2\varepsilon_{\max}} \right)^{1/\gamma} \quad (1.5)$$

A value of the critical exponent can vary from $\gamma = 1$ for purely normal ferroelectrics, to $\gamma = 2$, for purely relaxor ferroelectrics.⁸ The diffuseness parameter is an empirical value that describes the width of the diffuse phase transition.

The relatively rapid decrease of the polarization to zero found in normal ferroelectrics at T_c is much more gradual in relaxor ferroelectrics. This gradual decrease extends to temperatures above T_{\max} before reaching zero. This can be observed in dielectric hysteresis loops. At temperatures below T_{\max} , relaxors show typical P-E hysteresis; however, the loops decay slowly into non-linearity as the temperature increases through the Curie range.

The local symmetry of the nano-domains in relaxors is typically rhombohedral. Because of the scale of the nano-domains, optical birefringence and x-ray diffraction measurements do not show anisotropy or line splitting, even far below T_{\max} . The global symmetry of relaxors is generally reported as pseudo-cubic, even in the polar state, due to this ambiguity.



ลิขสิทธิ์มหาวิทยาลัยเชียงใหม่
Copyright © by Chiang Mai University
All rights reserved

Table 1.1 Property difference between relaxor and normal perovskite ferroelectrics.⁷

Property	Normal ferroelectric	Relaxor ferroelectric
Permittivity temperature dependence $\epsilon = \epsilon(T)$	Sharp 1 st or 2 nd order transition about Curie temperature (T_c)	Broad-diffuse phase transition about Curie maxima (T_{max})
Permittivity temperature and frequency dependence $\epsilon = \epsilon(T, \omega)$	Weak frequency dependence	Strong frequency dependence
Permittivity behavior in paraelectric range ($> T_c$)	Follow Curie-Weis law Equation $1/K = (T - \theta_c)/C$	Follow Curie-Weis square law Equation: $1/K = 1/K_{max} + (T - T_{max})^2 / 2K_{max}\delta^2$
Remanent polarization	Strong remanent polarization	Weak remanent polarization
Scattering of light	Strong anisotropy (birefringent)	Very weak anisotropy to light (pseudo-cubic)
Diffraction of x-rays	Line splitting owing to spontaneous deformation from paraelectric to ferroelectric phase	No x-ray line splitting giving a pseudo-cubic structure

1.2.3 Relaxor ferroelectric modeling.

Many theories have been proposed to explain the behavior of relaxor ferroelectrics. While each theory explains a particular feature of relaxors, none completely describes all of their behavior. The most widely accepted model is based on the works of Smolenskii⁹, Cross⁵, and Randall and Bhalla.¹⁰

The theory proposed by Smolenskii⁴ in 1958 stated that the diffuseness of the phase transition (DPT) was due to compositional fluctuations on a microscopic scale on the order of 100-1,000 Å. He observed that DPTs were observed in systems such as $\text{Pb}(\text{Mg}_{1/3}\text{Nb}_{2/3})\text{O}_3$ [PMN], $\text{Pb}(\text{Ni}_{1/3}\text{Nb}_{2/3})\text{O}_3$ [PNN] and $(\text{Ba},\text{Sr})(\text{Ta},\text{Nb})_2\text{O}_6$, but not in solid solutions such as BaTiO_3 - SrTiO_3 [BT-ST] and SrTiO_3 - PbTiO_3 [ST-PT]. Based on this observation, the diffuseness was due to local ordering on a submicroscopic level. This local ordering, on the order of 100-200 Å, of cations on either the A or B-site of the sub lattice, results in each region having a different Curie temperature. On a macroscopic scale, the statistical variation in Curie temperatures results in a broad ferroelectric to paraelectric phase transition. In 1970, Smolenskii⁹ explained this theory by discussing the origin and stability of the diffuse phase transition region. He postulated that relaxor ferroelectrics are made up of polar and non-polar regions, whose relative amounts determine the magnitude of the DPT. If one considers the cooling of the relaxor from far above T_{max} , the maximum in the dielectric constant, the material will consist of small isolated polar regions in a non-polar matrix. As the material further is cooled, nucleations of new polar regions and growth of existing regions continue. At still lower temperatures, the polar regions reach a size that enable them to make contact and begin forming domain walls. At the temperature of maximum dielectric constant, T_{max} , the volume fraction of the polar

and non-polar phases is equal. At $T < T_{\max}$, the polar domain structure grows and the non-polar regions become smaller and eventually isolated.

The relaxor ferroelectric properties closely depend on the degree of order/disorder and the scale or coherent length of the ordered nanodomains. For the lead-based complex perovskites $\text{Pb}(\text{B}'\text{B}'')\text{O}_3$, the order/disorder depends both on the valence and ionic radii differences of the two cations on the B-sites. Three scenarios may be possible.

(i) The chemical difference between B' and B'' are large enough for the cations to order and thereby to form the superstructure, as in the case of the ordered $\text{Pb}(\text{Co}_{1/2}\text{W}_{1/2})\text{O}_3$ and $\text{Pb}(\text{Mg}_{1/2}\text{W}_{1/2})\text{O}_3$ with elpasolite-type structure. This type of long-range order is of long coherence and usually results in normal ferro- anti-ferroelectric phase transitions.

(ii) Some complex $\text{Pb}(\text{B}'\text{B}'')\text{O}_3$ compounds like $\text{Pb}(\text{Sc}_{1/2}\text{Ta}_{1/2})\text{O}_3$ [PST] $\text{Pb}(\text{Sc}_{1/2}\text{Nb}_{1/2})\text{O}_3$ and $\text{Pb}(\text{In}_{1/2}\text{Nb}_{1/2})\text{O}_3$, the chemical differences between B' and B'' are close to the critical limit for B-site disorder/order occupancy so that it is possible to modify the degree of the ordering by appropriate thermal annealing (Figure 1.3), quenching or crystal growth conditions. Phenomenon initially studied in $\text{Pb}(\text{Sc}_{1/2}\text{Ta}_{1/2})\text{O}_3$ [PST] by Stenger and Setter¹¹ has been extensively investigated. With an increasing degree of order, the coherence length increases and a transition into normal ferroelectric take place (Figure 1.3). Since the B-side order in there compounds is compatible with the normal 1:1 ratio for B':B'', the stoichiometry is preserved and the ordering may be complete.

(iii) The Complex compounds $\text{Pb}(\text{B}'_{1/3}\text{B}''_{2/3})\text{O}_3$ like $\text{Pb}(\text{Mg}_{1/3}\text{Nb}_{2/3})\text{O}_3$, appear to be particularly interesting as for their nanostructure. With smaller chemical differences, the B' and B'' ions usually exhibit a long-range disordered occupancy. However the presence of one by one order between the Mg^{2+} and Nb^{5+} ions was actually revealed by means of electron microscopy (HRTEM). There long-range ordered nanodomains with a size of a few 100s Å and a shot coherence length are characteristic of relaxor ferroelectrics. Since the 1:1 order with composition $\text{Pb}(\text{Mg}_{1/3}\text{Nb}_{2/3})\text{O}_3$ does not match the 1:2 nominal ratio, the ordered domains are non-stoichiometric and negatively charged (Mg^{2+} -rich). They form an array of clusters spread inside a disordered matrix which must be positively charged due to an excess in Nb^{5+} , the average composition remaining the nominal formula $\text{Pb}(\text{Mg}_{1/3}\text{Nb}_{2/3})\text{O}_3$. The mean size of the ordered nanodomains was determined to be about 2nm. The volume fraction of the ordered nanodomains may reach about 1/3. The composition of the disordered Nb^{5+} -rich regions is close to $\text{Pb}(\text{Mg}_{1/3}\text{Nb}_{3/4})\text{O}_3$.

Figure 1.4 shows that the macroscopic behavior of the complex perovskites is closely related to the order/disorder nanostructures, and the relaxor ferroelectric exhibit not only B-site disorder regions, but also ordered nanoclusters with shot correlation length between them.

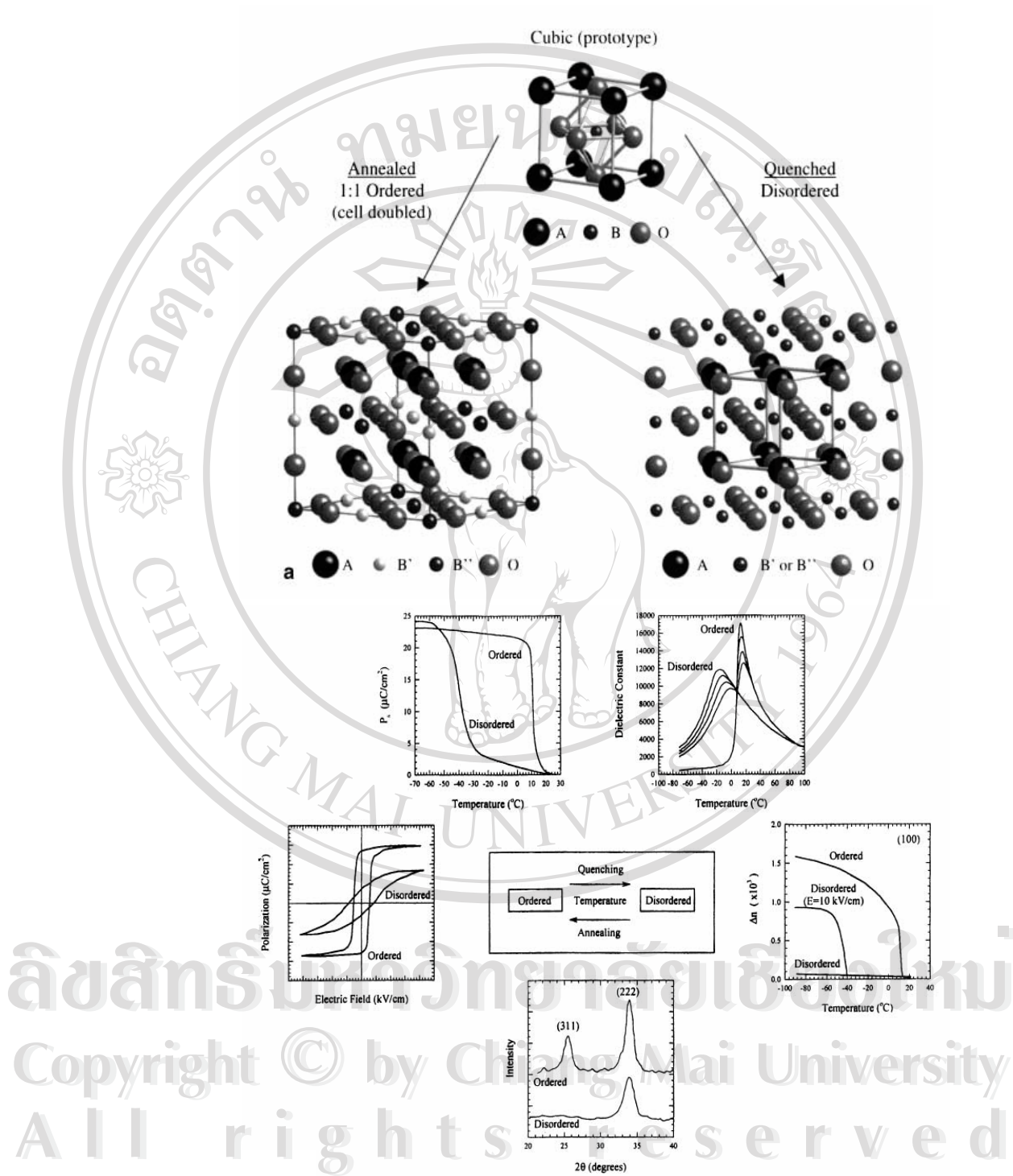


Figure 1.3 Differences between ordered and disordered $\text{Pb}(\text{Sc}_{1/2}\text{Ta}_{1/2})\text{O}_3$.¹²

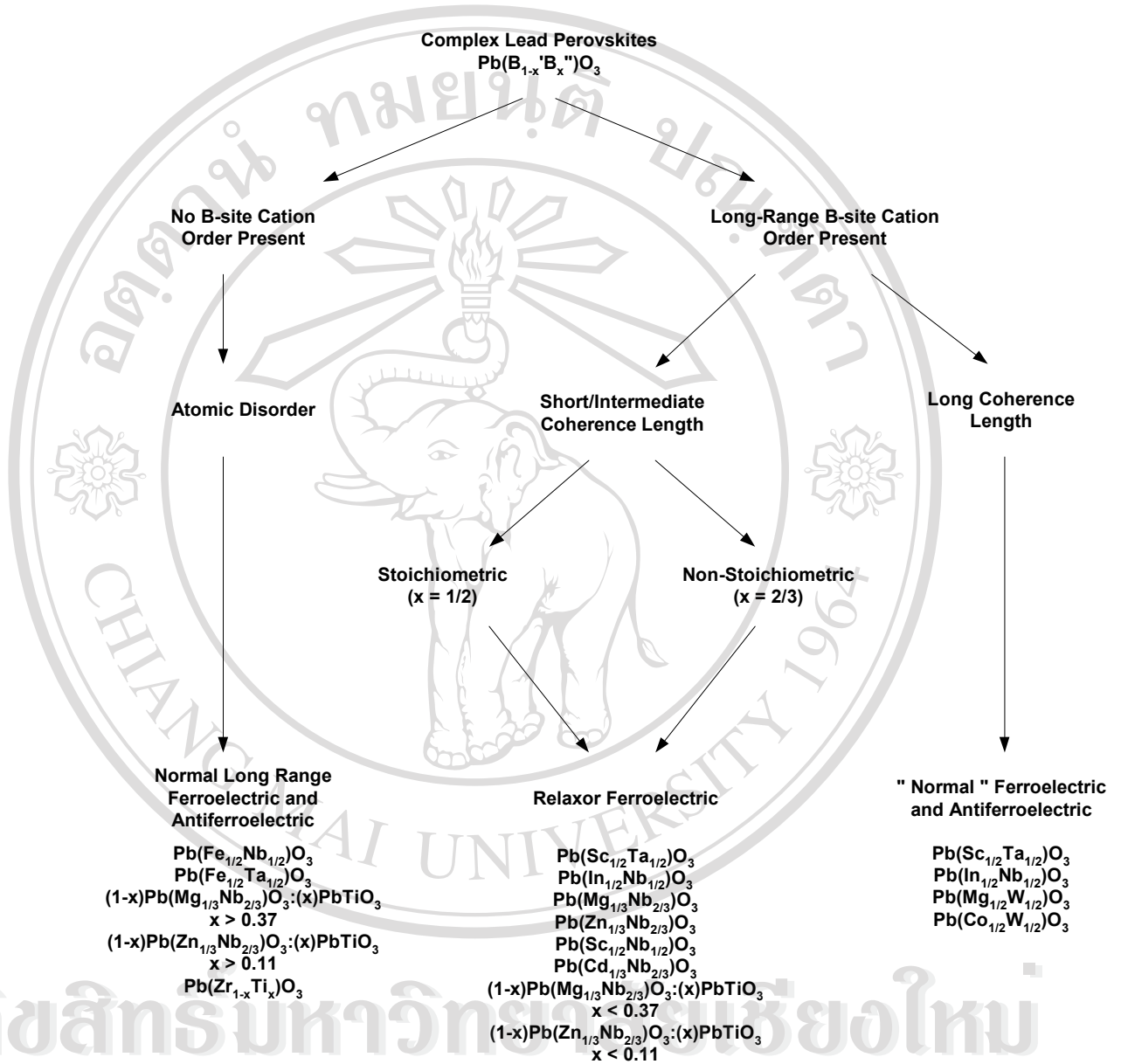


Figure 1.4 Various relaxor perovskite combinations and their classification based on short and long range ordering.¹⁰

1.3 Perovskite materials

1.3.1 Introduction

The perovskite structure is one of the most technologically important structure types in material science.^{6,13} Members of the perovskite family include relaxor ferroelectrics, superconductors, microwave dielectrics, magnetic materials, magneto-resistive materials, non-linear optical materials, catalysts, and thermoelectric materials.¹⁴ Furthermore, the vast majority of technologically important ferroelectric/piezoelectric materials belong to the perovskite family. The following sections describe the crystal structure and phase stability for oxide perovskite structures.

1.3.2 Crystal structure

The perovskite structure is named after the mineral calcium titanate, CaTiO_3 . However, the cubic (isometric) perovskite structure is better described by SrTiO_3 .¹⁴ Cubic SrTiO_3 has a space group, $Pm\bar{3}m$, with the titanium atoms located at the corners of the unit cell cube, the strontium atoms at the center of the cube, and the oxygen atoms placed at the centers of the twelve cube edges. This arrangement consists of orthogonal corner-shaped TiO_6 octahedra. There are other equally accurate ways to visualize the structure. The first alternative is a cubic cell that has the titanium atom at the center, the strontium atoms on the cell corners and the oxygen atoms on the cell faces (Fig. 1.5). This arrangement leads to the same orthogonal corner-shaped TiO_6 octahedra as described previously; however, only one unit cell is required to describe the octahedra, as opposed to multiple cells in the first case. One can visualize the

structure as a cubic close-packed structure in which the strontium and oxygen atoms are stacked in cubic close-packed layers in the [111] direction. The titanium atoms then fill in the octahedral holes. The structure formula is often referred to as:



in which the A atoms are in 12-fold coordination, and both the B atoms are in 6-fold coordination.

The perovskite structure can tolerate an enormous range of compositional modifications. The anions and cations in the perovskite structure can be interchanged with ions of different valences, as long as charge neutrality is maintained. The first of the three major variations is the $A^{1+}B^{5+}O_3$ family, an example of which is KNbO_3 . The best studied family is probably $A^{2+}B^{4+}O_3$, which includes PbTiO_3 and BaTiO_3 . Lastly, the $A^{3+}B^{3+}O_3$ family includes BiFeO_3 and BiScO_3 .

In addition to these three families, there is a wide variety of complex perovskite forms resulting from multiple ionic substitutions. Many of the materials in the complex perovskite family are known to be relaxor ferroelectric. The general formula for the complex perovskite is;



The A' and A'' cation sites typically contain Pb^{2+} , Ba^{2+} , Sr^{2+} , Bi^{3+} or La^{3+} ; the X anion site is generally occupied by oxygen; and the B' and B'' cation sites can contain a great variety of cations. The B' is usually occupied by a lower valence

cation such as Mg^{2+} , Ni^{2+} , Zn^{2+} , Fe^{3+} and Sc^{3+} . The B'' site cations are typically highly-charged ions such as Ti^{4+} , Nb^{5+} , Ta^{5+} and W^{6+} .

These substitutions generally lead to three major complex perovskite sub-families: $\text{A}^{2+}(\text{B}_{1/2}^{3+}\text{B}_{1/2}^{5+})\text{O}_3$, $\text{A}^{2+}(\text{B}_{1/2}^{2+}\text{B}_{1/2}^{6+})\text{O}_3$, and $\text{A}^{2+}(\text{B}_{1/3}^{2+}\text{B}_{2/3}^{5+})\text{O}_3$. Most relaxor ferroelectrics are rhombohedral perovskite, however, in many cases the symmetry is described as pseudo-cubic due to a lack of long-range global order.¹⁵

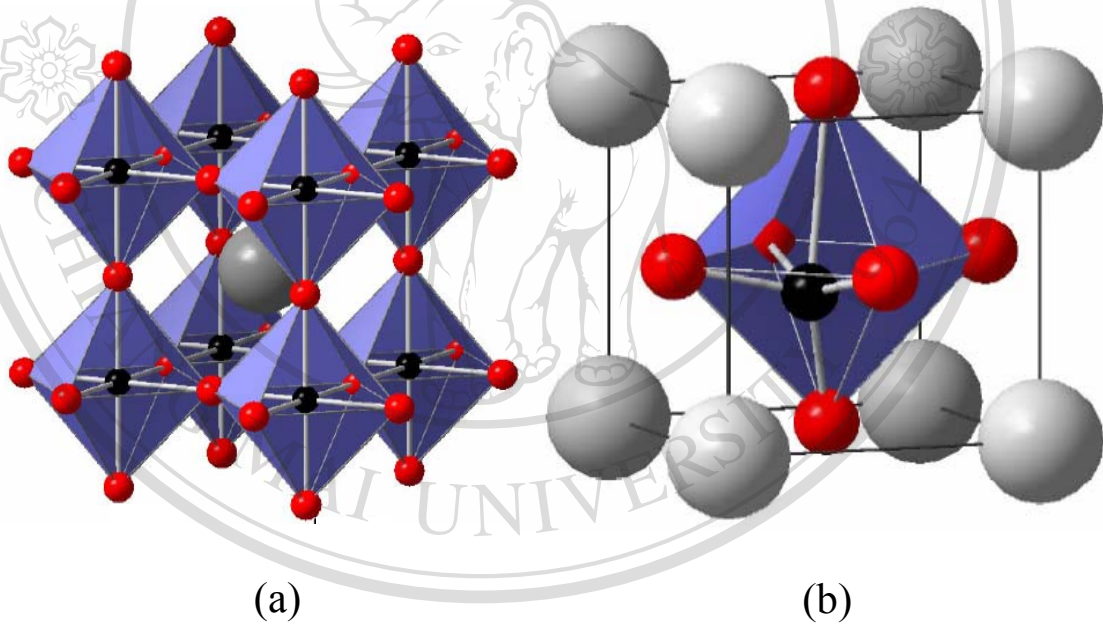


Figure 1.5 (a) three-dimensional network of BO_6 octahedra and

(b) an ABO_3 perovskite-type unit cell.

1.3.3 Tolerance factor and phase stability

Due to the large number of substitutions that are possible in the perovskite structure, Goldschmidt developed a “tolerance” factor to describe the stability limits of the structure. In an ideal cubic perovskite constructed of rigid spheres, each cation is large enough to be in contact with an oxygen anion, and the radii of the ions can be related via:^{16,17}

$$r_a + r_o = \sqrt{2}(r_b + r_o) \quad (1.8)$$

where, r_a , r_b and r_o are the ionic radii of the A-site and B-site cations, and the oxygen ion respectively (for values of the ionic radii see Shannon¹⁷).

However, in a real structure, the ions are not rigid, and as the A cation decreases in size, a point arrives when it is too small to remain in contact with the anions in the cubic structure. Therefore, the B-O-B bonds bend slightly by tilting the BO_6 octahedra to bring some anions into contact with the A cations. To allow for this distortion, a constant, t , is introduced into the above equation, thus:

$$r_a + r_o = t\sqrt{2}(r_b + r_o)$$

$$t = \frac{(r_a + r_o)}{\sqrt{2}(r_b + r_o)}$$

This constant is known as the tolerance factor and can be used as a measure of the degree of structural distortion compared to the ideal cubic perovskite structure. Using a rigid ion model, the ideal cubic perovskite structure has all ions in contact and a tolerance factor equal to 1. For a stable perovskite structure, the tolerance factor should be within the range of $0.8 < t < 1.05$.¹⁶ Generally, perovskites with tolerance factors larger than 0.98 are tetragonal and those with tolerance factors less than 0.97 are rhombohedral. This simple, but powerful, geometric argument alone is not always enough to describe the stability of the perovskite.

Since most perovskites contain lead and barium there is a tendency toward A-O bonding with a strong covalent character. This factor must be considered in determining the stability of the perovskite structure. The percentage of the ionic character of the bonds is proportional to the electronegativity difference between the cation and anion. Halliyal *et al.*¹⁸ developed a structure field map based on the average electronegativity difference between cations and the geometric tolerance factor (Fig. 1.6). The electronegativity differences of cation A and oxygen X_{A-O} and cation B and oxygen X_{B-O} were calculated using Pauling's electronegativity scale.

For $A(B'B'')O_3$ type perovskites, a weighted average value was used for calculating r_b and X_{B-O} . The electronegativity difference (ΔEN) is given by the following equation:

$$\Delta EN = \frac{(X_{A-O} + X_{B-O})}{2} \quad (1.9)$$

As shown in Fig. 1.6, Halliyal *et al.*¹⁸ observed that larger average electronegativity differences led to more stable perovskites, probably due to increased ionic bonding. This plot gives some insight as to why a material like PMN is more difficult to process than SrTiO₃, even though they have similar tolerance factors. BT and KNbO₃ both have high tolerance factors and electronegativity differences, which indicate strong ionic bonding in these compounds. Therefore, these compounds should form stable perovskite structures, as they are known to do.

Although CaTiO₃ has a slightly lower tolerance factor ($t \sim 0.97$), it forms a stable perovskite probably because of a large fraction of ionic bonding.

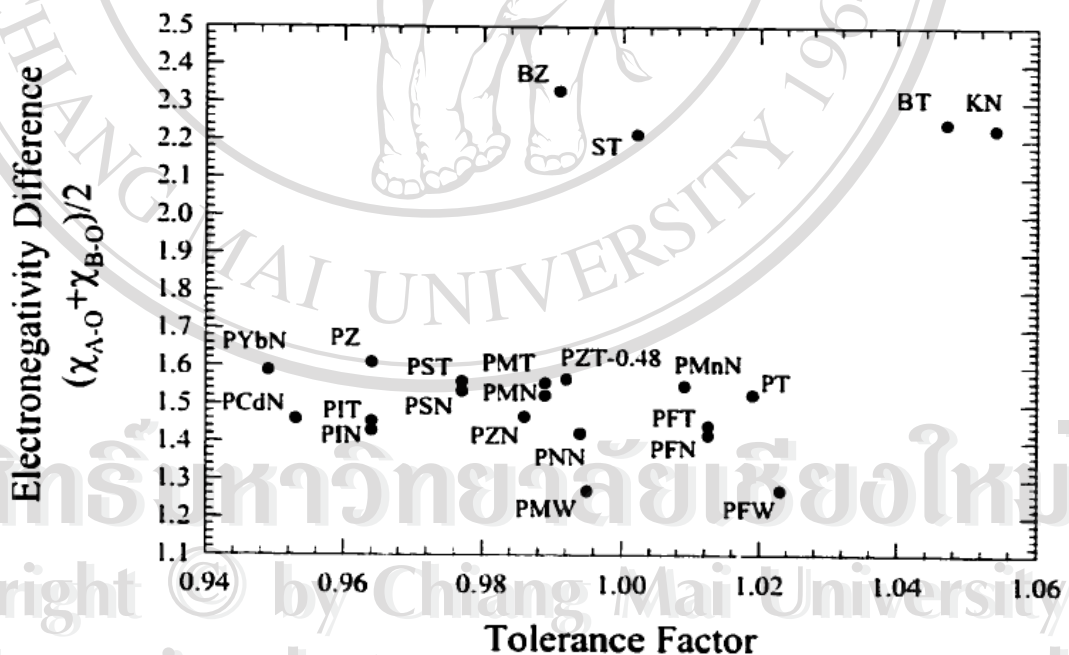


Figure 1.6 Structure-Filed map for various perovskite materials based on electronegativity difference and tolerance factor.¹⁸

For PbO-based $A(B'B'')O_3$ perovskite compounds, the electronegativity difference is small, and in most of the complex compounds the tolerance factor is considerably less than one. Therefore complex compounds are less stable compared to other perovskites. This observation agrees quite well with experimental data regarding the ease of compound preparation within perovskite structure. However, most of these compounds have relaxor ferroelectric properties, and their numerous synthesis routes have been attempted. Nevertheless, there have been no reports as yet on the synthesis of several important compounds by conventional solid state reactions, including $Pb(Zn_{1/3}Nb_{2/3})O_3$ (PZN), $Pb(Zn_{1/3}Ta_{2/3})O_3$ (PZT), $Pb(Ca_{1/3}Nb_{2/3})O_3$ (PCN), and $Pb(Ni_{1/2}W_{1/2})O_3$ (PNW), $Pb(Zn_{1/2}W_{1/2})O_3$ (PZW), $Pb(Ca_{1/2}W_{1/2})O_3$ (PCW), $Pb(Y_{1/2}Nb_{1/2})O_3$ (PYN) and $Pb(Er_{1/2}Nb_{1/2})O_3$ (PEN). Experimentally, the relative ease of lead-based perovskite fabrication roughly follows the following sequence



In other words, PZN is the most difficult relaxor perovskite to prepare in single-phase perovskite form. In fact, it is well-known that the PZN perovskite cannot be fabricated by conventional mixed oxide ceramic processing. However, this sequence is not a perfect fit to empirical data. For compounds such as PZ and PZN, other factors should be considering such as bonding and structural parameters, cation valence stability, ordering parameters, electron configuration, etc.

1.3.4 Columbite-(wolframite) Precursor Method

It is well-known that if the ceramic preparation of $\text{Pb}(\text{B}'\text{B}'')\text{O}_3$ perovskite is carried out by conventional mixed oxide processing, formation of stable, lead-based pyrochlore-type phases invariably occurs.¹⁶ The pyrochlore phases severely degrade the dielectric properties and are the primary cause of the variation in dielectric properties reported in the literature for any given relaxor composition.¹⁹ To obtain a stoichiometric perovskite PMN, a prototype of lead based complex perovskite, Swartz and Shrout²⁰ concluded that the intermediate pyrochlore phase reaction must be eliminated. To achieve this, a novel approach was devised whereby the two refractory B-site oxides, MgO and Nb_2O_5 , were pre-reacted with PbO, as shown below:²⁰



In this reaction sequence the pyrochlore formation is bypassed, leading to the direct formation of PMN. Preparations by this method always show substantial improvement in the amount of perovskite phase compared to conventional mixed oxide processing. It has been shown that PMN with a complete perovskite phase can be prepared easily by this method. The process of pre-reacting the B-site cations to form either a columbite $\text{B}_1(\text{B}_2)_2\text{O}_6$ or wolframite $\text{B}_1\text{B}_2\text{O}_4$ has been successfully applied to many other relaxors: PNN, PFN, PMT and PST. This method, however, was only partially successful for PIN and totally unsuccessful for a number of other relaxors such as PZN, PCN and PZT.¹⁶

1.4 Morphotropic Phase Boundaries (MPB) in normal and relaxor ferroelectric solid solutions

1.4.1 Introduction

Piezoelectric ceramics of perovskite lead zirconate-titanate, $\text{Pb}(\text{Zr}_x\text{Ti}_{1-x})\text{O}_3$ (PZT) have been extensively investigated since their discovery in the 1950's.² Owing to the exceptionally good dielectric and piezoelectric properties as well as high Curie temperature ($> 350^\circ\text{C}$), PZT composition, which is usually modified with acceptors or donors, has important technological applications as piezoelectric transducers, pyroelectric detectors, electro-optic devices, and induced charge release devices.²¹

Lead titanate (PbTiO_3) and lead zirconate (PbZrO_3) are soluble in all proportions. When the titanium cation (Ti^{4+}) in PbTiO_3 is partially substituted with zirconium (Zr^{4+}) the tetragonal distortion of the unit cell of PbTiO_3 is reduced. With more than half of the Ti^{4+} cations replaced by Zr^{4+} , the structure of the solid solution becomes rhombohedral. The phase diagram between the tetragonal and rhombohedral phases is almost temperature independent up to the Curie temperature, above which, the cubic paraelectric structure exists. Polycrystalline ceramics, with compositions near the morphotropic phase boundary (MPB), have exceptionally high dielectric constants and piezoelectric-related coefficients. This is believed to be due to the increased number of domain orientations caused by the field-enforced switching between the tetragonal and rhombohedral phases during the poling process of the ceramic. The phase diagram of the PZT system is shown in Fig 1.7. At a temperature above T_c , the ideal cubic para-electric structure ($Pm3m$) is stable. Below T_c , PZT is ferroelectric and shows, for Ti-rich compositions ($0 \leq x \leq 0.52$), a tetragonal distortion

of the unit cell ($P4mm$). Compositions with lower Ti content ($0.52 \leq x \leq 0.94$) have a rhombohedrally distorted unit cell.

Alternate MPB systems can be found in relaxor-PbTiO₃, also shown in Fig. 1.7. A compilation of these relaxor materials and their solid solutions have been organized by Landolt-Bornstein and numerous MPB systems have been reported.²² Early investigations of relaxor - PT in the 1960s and 1970s were plagued with inadequate process controls resulting in piezoelectric ceramics of marginal interest.²³ With the advent of the columbite precursor method and an overall understanding of the perovskite-pyrochlore phase stabilities and their corresponding structure-property relationships, a renewed interest in the Relaxor - PT MPB systems came about. To achieve even better dielectric and piezoelectric properties, MPB - based ceramics are engineered further by compositionally adjusting the Curie temperature (T_c) downward in relation to room temperature. This enhanced effect comes with the expense of greater temperature dependence to the properties, a lessened stability of the polarization stability, leading to aging and loss of piezoelectric activity. The wide range of Relaxor-PT systems has been recently reviewed, including their piezoelectric and dielectric properties. The most commonly investigated MPB compositions are depicted in this diagram. The diagram shows three morphotropic phase boundaries, the one already discussed on the PZ-PT system (MPB I), and the other on the relaxor-PT systems (MPB II), this composition has attracted considerable interest because of their potential for electromechanical applications.

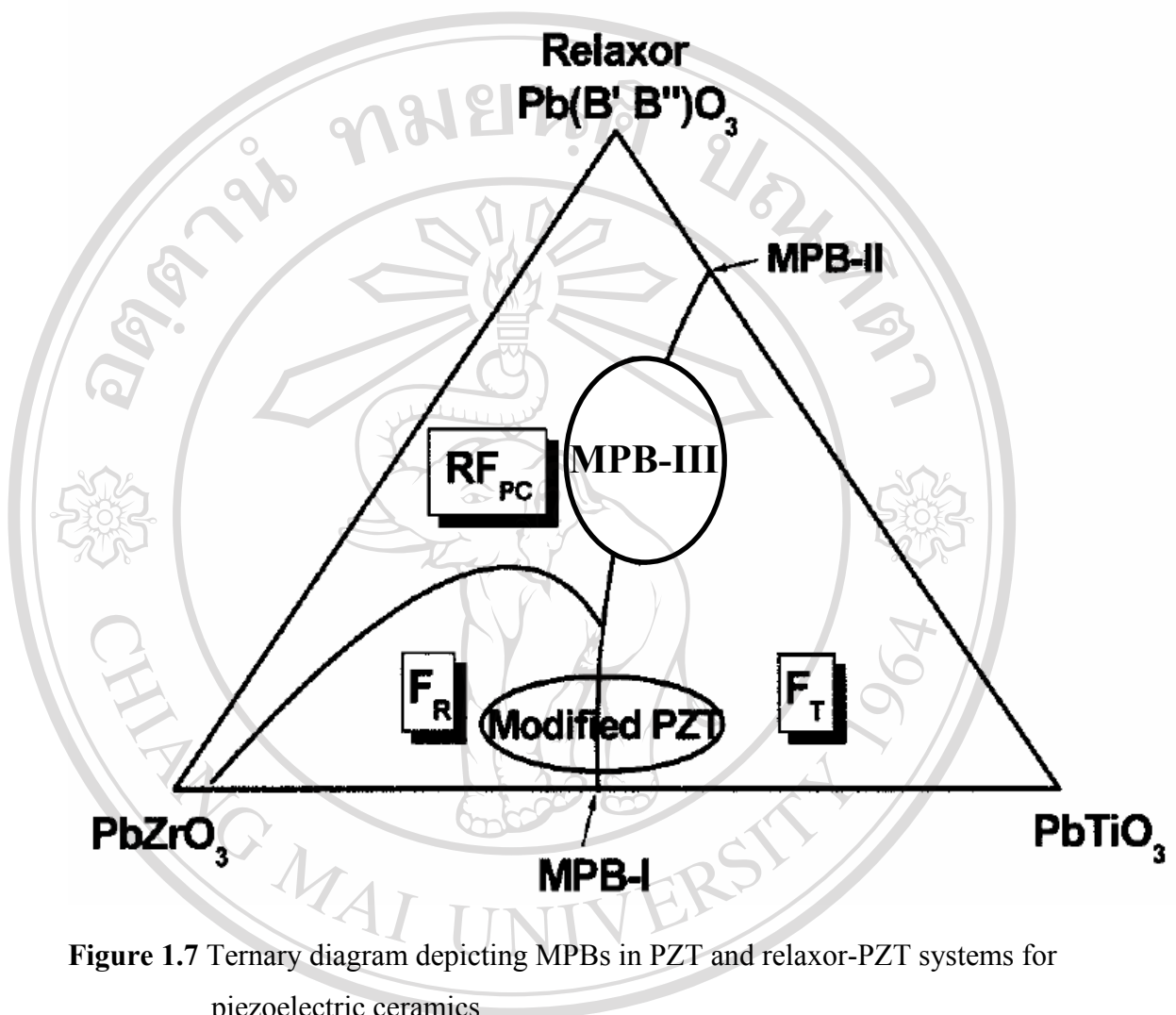


Figure 1.7 Ternary diagram depicting MPBs in PZT and relaxor-PZT systems for piezoelectric ceramics.

The last MPB (MPB III) has also been previously studied and is well defined, which is located near a typical relaxor/PZT ratio of 50/50.²⁴ In contrast to the PZT system, the amount of PT associated with relaxor-PT MPB is, in general, less than that for PZT and varies between 7% for PFN-PT to 50 mol% for PYN-PT. In the PZT system, the MPB is relatively insensitive to temperature. However, in most relaxor-PT systems, the MPB composition is strongly dependent.

1.4.2 Stabilization of the perovskite phase in PZN ceramic solid

solutions.

$\text{Pb}(\text{Zn}_{1/3}\text{Nb}_{2/3})\text{O}_3$ (PZN) is an important relaxor ferroelectric material with the rhombohedral structure at room temperature. A diffuse phase transition from the paraelectric state to a ferroelectric polar state occurs at 140°C .²⁵ Extensive research has been carried out on PZN single crystals because of their excellent dielectric, electrostrictive, and optical properties.²⁶ The solid solution between PZN with a rhombohedral system and PbTiO_3 (PT) with tetragonal symmetry has a morphotropic phase boundary near 9 mol% PT.²⁵ Single crystals with a composition near the MPB show extremely large dielectric ($\epsilon_r \sim 60,000$) and piezoelectric coefficients, and are much larger than those of PZT ceramics. Single crystals of the MPB composition (0.91PZN-0.09PT) display one of the highest electromechanical coupling factors (0.92) and piezoelectric coefficients (1500 pC/N) at room temperature.²¹ Because of the high Curie temperature and the low sintering temperature ($1050\text{-}1100^\circ\text{C}$), PZN-based compositions are promising ferroelectrics for device applications.

Although single crystals of PZN can be routinely grown by the flux method, it is known that perovskite PZN ceramics cannot be synthesized by the conventional mixed-oxide method without doping.^{18,27,28} Attempts to synthesize perovskite PZN ceramics invariably results in the formation of a pyrochlore phase with accompanying degradation of the dielectric and piezoelectric properties. When the normal solid state reaction is carried out to prepare PZN, a mixture of perovskite PZN and pyrochlore-type $\text{Pb}_3\text{Nb}_4\text{O}_{13}$ or $\text{Pb}_2\text{Nb}_2\text{O}_7$ is formed.²⁹ The anion-deficient, cubic pyrochlore, $\text{Pb}_3\text{Nb}_4\text{O}_{13}$, is the most common; however, both phases can be present. $\text{Pb}_2\text{Nb}_2\text{O}_7$ is a

rhombohedral pyrochlore that is also sometimes present. The pyrochlore phase is undesirable because of its relatively low dielectric constant (~ 200) and non-piezoelectric nature.

A reaction sequence for pyrochlore formation in PMN has been proposed by Lejeune *et.al.*³⁰ In this reaction, PbO and Nb₂O₅ react first to form cubic pyrochlore. Further reaction with PbO results in the formation of a rhombohedral pyrochlore. At high temperatures, the rhombohedral pyrochlore reacts with MgO to form perovskite PMN, with the reappearance of cubic pyrochlore. A similar reaction is believed to occur in PZN-based ceramics.³¹

It is also difficult to prepare several other relaxor materials, including Pb(Mg_{1/3}Nb_{2/3})O₃ in ceramic form, without the formation of the pyrochlore phase.¹⁶ By adopting a different processing scheme, it is possible to overcome the problem of pyrochlore formation in PMN ceramics.²⁰ In this method, MgO is pre-reacted with Nb₂O₅ to form MgNb₂O₆, which has the columbite structure. MgNb₂O₆ is then reacted with PbO to obtain phase pure perovskite PMN ceramic. Since Mg²⁺ and Zn²⁺ have the same charge and approximately similar ionic radii¹⁷, it seems possible to prepare PZN ceramics using the similar technique of first preparing columbite ZnNb₂O₆ by reacting ZnO and Nb₂O₅ and subsequently reacting ZnNb₂O₆ with PbO. However, the reaction product obtained by this reaction sequence is a pyrochlore phase.¹⁶ There have been many attempts to stabilize the perovskite structure in PZN and PZN-PT ceramics by the use of compositional modifications. Since barium titanate has the largest electronegativity difference and tolerance factor it should be possible to stabilize PZN or PMN in perovskite form by adding a small percentage of BaTiO₃. Belsick *et.al.*²⁸ indicated that the addition of 6-7 mol% BaTiO₃ or 10 mol%

SrTiO₃ is sufficient to stabilize the perovskite phase in PZN. Both BT and ST were determined as the best additives to stabilize the perovskite phase in the PZN-PT system by considering the thermodynamics of the system and the ionic nature of the chemical bonds. Furthermore, the perovskite structure in PZN can be stabilized by the addition of Ba(Zn_{1/3}Nb_{2/3})O₃³² as a third component or by the partial replacement of PbO with K₂O.³³

Moreover, efforts by several researchers to stabilize the perovskite structure in PZN or PZN-PT MPB compositions by the addition of other perovskite compounds or oxides have been more successful. Many of the compositions developed are promising for actuators and Multi-Layer Capacitors (MLC). A summary of the compositions and properties of different systems that have investigated is presented in Table 1.2.

Recently Fan *et al.*²⁴ showed that the perovskite phase of Pb(Zn_{1/3}Nb_{2/3})O₃ (PZN) ceramics was stabilized by adding a Ti-rich side tetragonal phase of Pb(Zr_{0.47}Ti_{0.53})O₃ (PZT) located across the morphotropic phase boundary (MPB). When 40% PZT was added, a rhombohedral perovskite phase was formed without any trace of the pyrochlore phase. The transition from rhombohedral to tetragonal phase was observed clearly from the XRD profile peak splitting with increasing PZT concentration. The rhombohedral phase fraction decreased markedly with increasing PZT concentration, as shown in Fig. 1.8.

Table 1.2 Composition and properties of PZN based ceramics.

Compositions	Composition range investigated	Range of Curie Temperature (°C) (T_{max})	Highest Dielectric Constant at $T_{(max)}$	References
x Pb _{1-y} K _y (Zn _{1/3} Nb _{2/3})O _{3-y/2} -(1-x)PT	$x = 0.8$ to 1.0 $y = 0.08$ to 0.15	50 - 200	5,500	33
PZN-BZN-PT		20 - 350	7,000	32
(1-x)PZN-xPT	$x = 0.0$ to 1.0	390	60,000	34
(1-x)PZN-xBT	$x = 0.0$ to 1.0	-130 - 140	13,500	28
(1-x-y)PZN-xBT-yPT	$x,y = 0.0$ to 0.2	-5 - 200	15,000	27
(1-x-y)PZN-xST-yPT	$x,y = 0.0$ to 0.2	-45 - 140	8,330	28
(1-x)PZN-xPNN	$x = 0.2$ to 1.0	-120 - 75	8,860	35
(1-x-y)PZN-xPNN-yPT	$x = 0.0$ to 0.4 $y = 0.0$ to 0.4		13,000	36
(1-x)PZN-xPZT(Zr/Ti 47/53)	0.2 to 0.8	200-300	22,000	24
(1-x)PZNMN -xST	$x = 0.12$			31
PZN,PMN-BT		5-20	13,000	37
0.85PZN-0.15 ATiO ₃ (A= Pb,Ca,Sr,Ba)			5,000	38

PZN : Pb(Zn_{1/3}Nb_{2/3})O₃; PNN : Pb(Ni_{1/3}Nb_{2/3})O₃; ST : SrTiO₃;

PMN : Pb(Mg_{1/3}Nb_{2/3})O₃; PZ : PbZrO₃; BZN : Ba(Zn_{1/3}Nb_{2/3})O₃;

BT : BaTiO₃

The 0.5PZN–0.5PZT specimen was found to have a coexistence of two phases, with a high piezoelectric coefficient of $d_{33} \sim 430$ pC/N, an electromechanical coupling factor of $k_p \sim 0.67$, a field-induced strain of $S_{33} \sim 0.24\%$ at 2 kV/mm, and a remnant polarization of $P_r \sim 27$ mC/cm².³⁹ A transition from a rhombohedral to tetragonal phase occurred when a relatively low electrical field was applied to the specimen. This transformation occurred only when the rhombohedral phase coexisted with an equal amount of the tetragonal phase.

Small rhombohedral domains, which were present around the relatively large tetragonal domains, were transformed as a result of the applied field. The excellent electromechanical properties at the MPB composition was attributed to this phase transition in the PZN based ceramics.

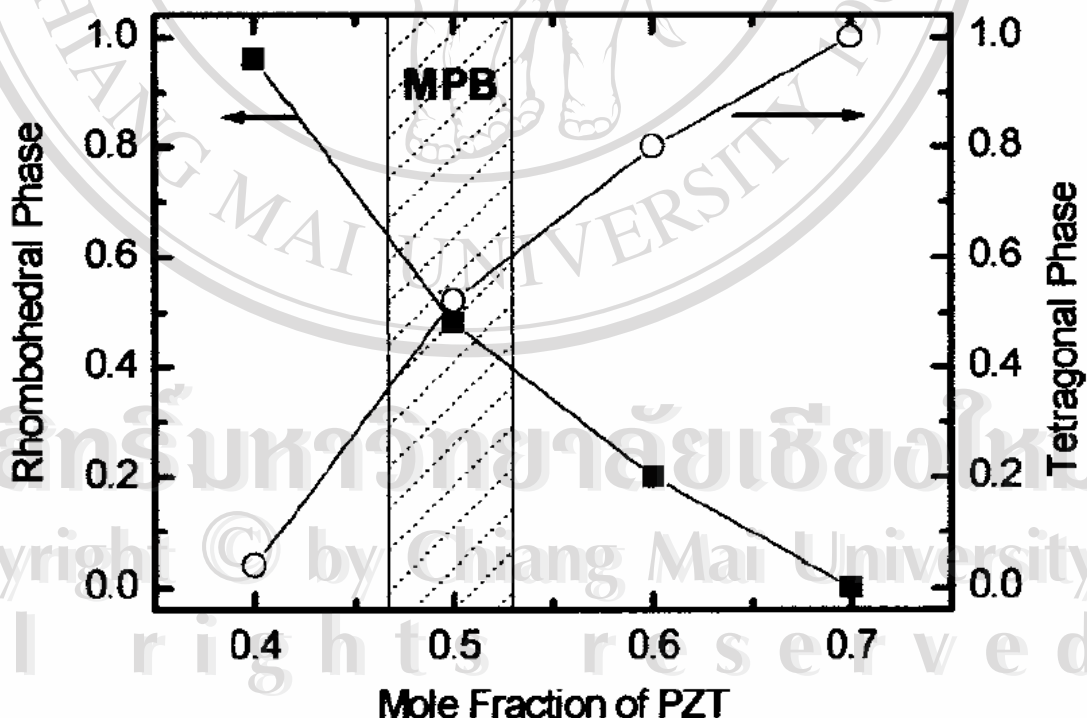


Figure 1.8 Relative concentration of the rhombohedral phase with respect to the tetragonal phase as a function of PZT content.²⁴

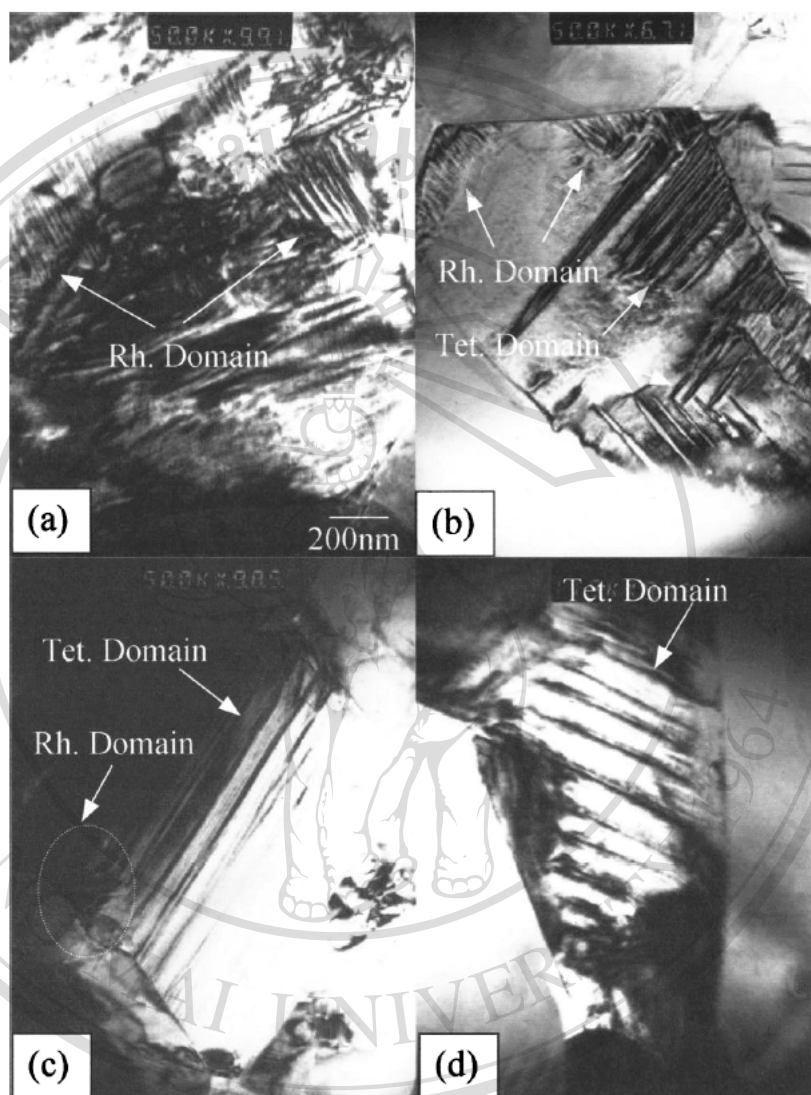


Figure 1.9 TEM micrographs of $(1-x)\text{PZN}-x\text{PZT}$ ceramics: (a) $x = 0.4$, (b) $x = 0.5$, (c) $x = 0.6$, (d) $x = 0.7$, showing the evolution of the tetragonal domains (Tet. Domain) and the rhombohedral domains (Rh. Domain).²⁴

Bright-field TEM images of $0.6\text{PZN} - 0.4\text{PZT}$, $0.5\text{PZN} - 0.5\text{PZT}$, $0.4\text{PZN} - 0.6\text{PZT}$ and $0.3\text{PZN} - 0.7\text{PZT}$ specimens are illustrated in Fig. 1.9. This demonstrates the evolution of the ferroelectric domain structure with the rhombohedral to tetragonal phase transformation.

Lenticular rhombohedral domains were observed in the $0.6\text{PZN} - 0.4\text{PZT}$ specimen as shown in Fig. 1.9(a). The lengths of these domains were less than 300 nm and their widths were approximately several hundred Å. The "plate-like" tetragonal domains were dominant with 180° domain walls in the $0.4\text{PZN} - 0.6\text{PZT}$ (Fig.1.9(c)) and $0.3\text{PZN} - 0.7\text{PZT}$ (Fig. 1.9(d)) specimens. Interestingly, the coexistence of the tetragonal and the rhombohedral domains are well illustrated by the TEM micrographs of the $0.5\text{PZN} - 0.5\text{PZT}$ specimen. The typical tetragonal domains, with 180° and 90° domain walls, are clearly shown in this micrograph. A closer examination of this micrograph indicates that there are small rhombohedral domains with 71° or 108° domain walls around the relatively large tetragonal domains. This TEM micrograph supports the XRD results given before. Therefore, a direct observation of the phase transition and ferroelectric domain realignment in this type of "two-phase coexistence zone" was made using XRD for both the fresh and poled $0.5\text{PZN} - 0.5\text{PZT}$ ceramic pellets.

From XRD data, dielectric data, and domain structures from the TEM images, it can be concluded that the MPB of this system which separates a tetragonal phase (PZT-rich) from a rhombohedral phase (PZN-rich) exists at the composition $x = 0.5$. Moreover, in the PZN-PZT system, when the Pb concentration is slightly less than the stoichiometric amount, a large amount of pyrochlore phase is formed together with the perovskite phase. On the other hand, an excessive amount of lead leads to the

formation of PbO on the surface of the specimen. These second phases are seriously detrimental to electromechanical properties. The effect of lead content on the phase evolution was also observed in the SEM micrographs. The microstructures of the $\text{Pb}_x((\text{Zn}_{1/3}\text{Nb}_{2/3})_{0.5}(\text{Zr}_{0.47}\text{Ti}_{0.53})_{0.5})\text{O}_3$ specimens with various lead contents are shown in Figs. 1.10(a) – (d). When the lead content was deficient ($x = 0.98$), the formation of pyrochlore phases (small diamond-shaped grains) in the relatively large perovskite grains was clearly observed, as shown in Fig. 1.10(a).

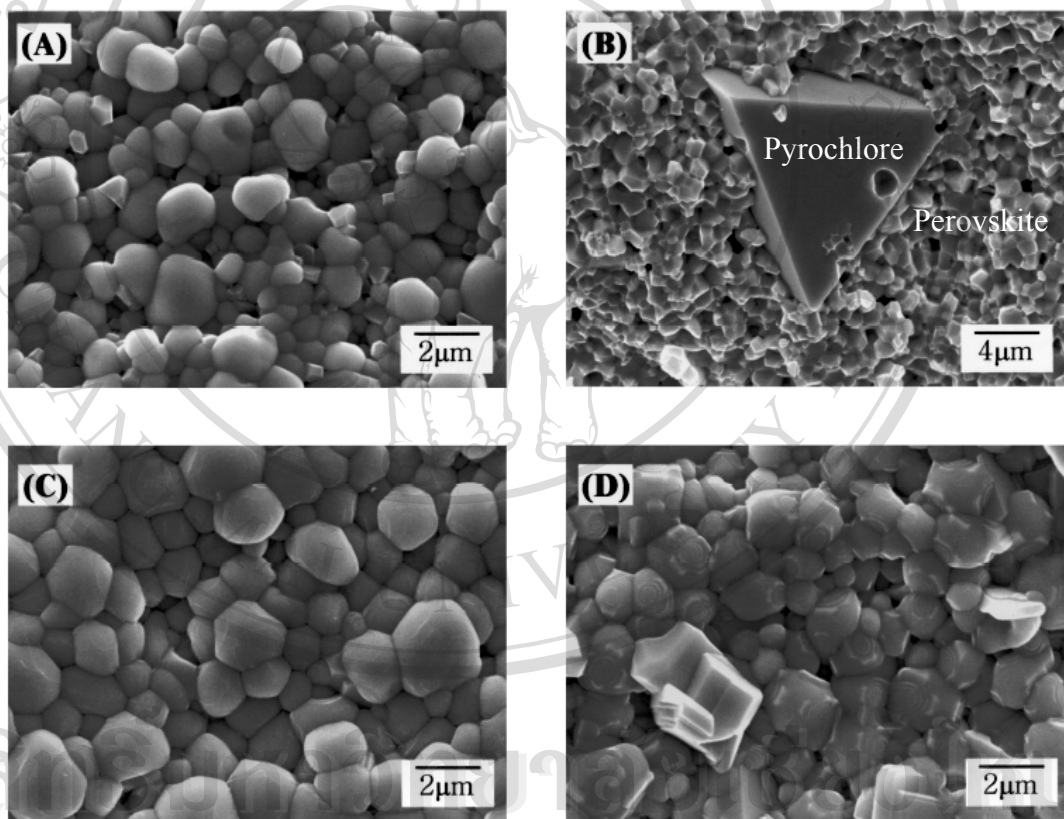


Figure 1.10 SEM micrographs of $\text{Pb}_x((\text{Zn}_{1/3}\text{Nb}_{2/3})_{0.5}(\text{Zr}_{0.47}\text{Ti}_{0.53})_{0.5})\text{O}_3$ ceramics: (a) free surface with $x = 0.98$, (b) fracture surface with $x = 0.98$, (c) free surface with $x = 1.01$, and (d) free surface with $x = 1.03$.²⁴

Inside the specimen, a larger pyrochlore phase was formed, as shown in the SEM micrograph on the fracture surface in Fig. 1.10(b). When the lead content was increased to $x = 1.01$, the microstructure became homogeneous, with no second phases (Fig. 1.10(c)). The micrograph in Fig. 1.10(c) also illustrates that the porosity was reduced markedly compared to the specimen in Fig. 2(a). When the lead content was increased further to $x = 1.03$, the surface morphology was changed again, as shown in Fig. 1.10(d). The formation of a second phase and the traces of a liquid phase were observed in this micrograph.

1.4.3 Characteristic features of ferroelectric $\text{Pb}(\text{Ni}_{1/3}\text{Nb}_{2/3})\text{O}_3\text{-Pb}(\text{Zr}_x\text{Ti}_{1-x})\text{O}_3$ ceramics

Lead nickel niobate ($\text{Pb}(\text{Ni}_{1/3}\text{Nb}_{2/3})\text{O}_3$ or PNN) was one of the first known relaxor ferroelectrics originally reported by Smolenskii and Agranovskaya.⁴ The first PNN single crystal showed typical relaxor ferroelectric behavior, with a room temperature dielectric constant of $\sim 2,500$ at 1 kHz, which increased to $\sim 4,000$ at the transition temperature ($T_{\text{max}} - 120^\circ\text{C}$). PNN crystals were grown in a platinum crucible containing a melt of PNN and PbO at a weight ratio of 2:3. Crystallization was achieved by cooling the melt from $1,200^\circ\text{C}$ at a rate of $20\text{-}40^\circ\text{C/h}$.⁴⁰ In 1983, Vetch⁴¹ showed that ceramics of phase-pure PNN could be prepared using the columbite precursor method. Single-phase perovskite PNN was prepared by the reaction of NiNb_2O_6 with PbO for 4 hours at $1,000^\circ\text{C}$. The calcined powder was pressed and sintered at $1,200^\circ\text{C}$ for 1 hour. X-ray diffraction (XRD) studies on ceramics that sintered under these conditions suggested the samples were single phase perovskite with cubic symmetry.

The $(1-x-y)\text{Pb}(\text{Ni}_{1/3}\text{Nb}_{2/3})\text{O}_3-(y)\text{PbZrO}_3-(x)\text{PbTiO}_3$ system was first investigated by Buyanova *et al.*⁴² In that study, PNN was added to the MPB composition of PZT to study the effect on the MPB. The most comprehensive study of the PNN-PZ-PT system was undertaken by Luff *et al.*⁴³ In that study, they identified large piezoelectric coefficients for the compositions PNN : PZ : PT ($z = 0.50, x = 0.15, y = 0.34$) ((PNNZT (50 / 15 / 34) and PNNZT (50.0 / 15.5 / 34.5)). In a series of papers by Kondo *et al.*⁴⁴, the location of the MPB was further refined. They showed that the composition (50 / 15.5 / 34.5) had some of the largest known electromechanical coupling factors ($k = 80\%$). Recently, E. F. Alberta⁴⁵ reported on the use of hot isostatic pressing (HIPing) to enhance the electrical and optical properties of PNNZT (50.0 / 15.5 / 34.5). The results showed that there were two additional anomalies in the dielectric properties present in the composition studied. Plotting the derivative allows one to discern the location of the two additional peaks, as shown in Fig. 1.11.

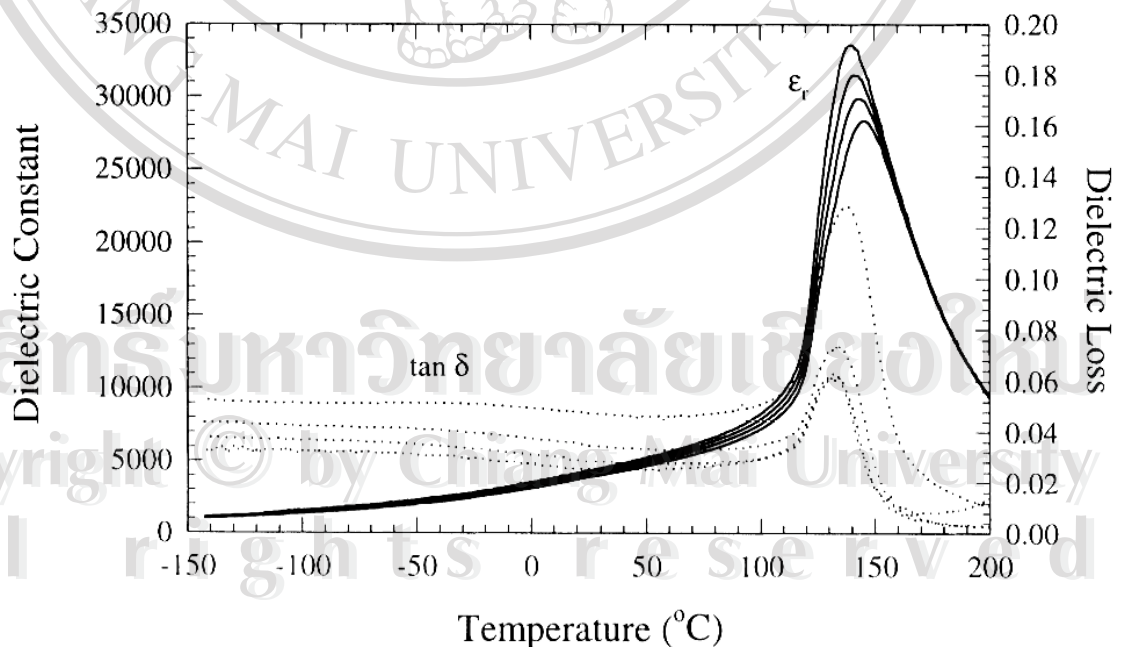


Figure 1.11 Temperature dependence of the dielectric constant and loss for PNNZT ceramics.⁴⁵

The first of these peaks is at 0 °C, and is due to a rhombohedral to tetragonal phase transition. The other is at 124 °C and is due to the tetragonal to pseudo-cubic phase transition. This phase transition has also been referred to as the normal ferroelectric to relaxor ferroelectric or macro- to nano-domain transition. Fig. 1.12(a) shows a typical well saturated hysteresis loop observed using an applied field of 75 kV/cm. The maximum polarization, remanent polarization and coercive field were 43.0 $\mu\text{C}/\text{cm}^2$, 33.3 $\mu\text{C}/\text{cm}^2$, and 5.46 kV/cm, respectively. The piezoelectric strain was also measured for the PNNZT ceramics. Fig. 1.12(b) illustrates the electric field dependence of the strain. The bipolar strain plot confirms the value of the coercive field of 5.5 kV/cm. The maximum strain realized by the ceramics was 0.29%.

After hot isostatic pressing at 1,100°C, the density increased to more than 99% and the grain size was 3.1 μm . Evidence of a macro- to nano-domain transition as well as a structural phase transition between the ferroelectric tetragonal and rhombohedral phases was suggested by the dielectric, piezoelectric, and pyroelectric experimental data. The room temperature dielectric constant value of 4,200 increased to 31,503 at 140°C (with a measuring frequency of 1 kHz).

Poling increased the room temperature dielectric constant to 5,940. Large piezoelectric coefficients, $d_{33} = 810$ pC/N and $d_{31} = -378$ pC/N, and $k_p = 69\%$, $k_{31} = 43\%$, $k_t = 56\%$, and $k_{33} \sim 80\%$, were measured at room temperature.⁴⁵ More recently, the B-site precursor method was developed and has been applied to prepare PNN-PZT ceramics, although in some cases it was not entirely successful. This method is based on the high-temperature synthesis of a precursor that contains all the B-site cations (Ti, Zr, Ni, and Nb). This synthesis yields a biphasic mixture that contains a ZrTiO_4 -like phase and a rutile-like phase. Based on dielectric permittivity versus temperature measurements and high-temperature XRD, a phase diagram for 40 mol% PNN in PZT was proposed by Rebert *et al.*⁴⁶

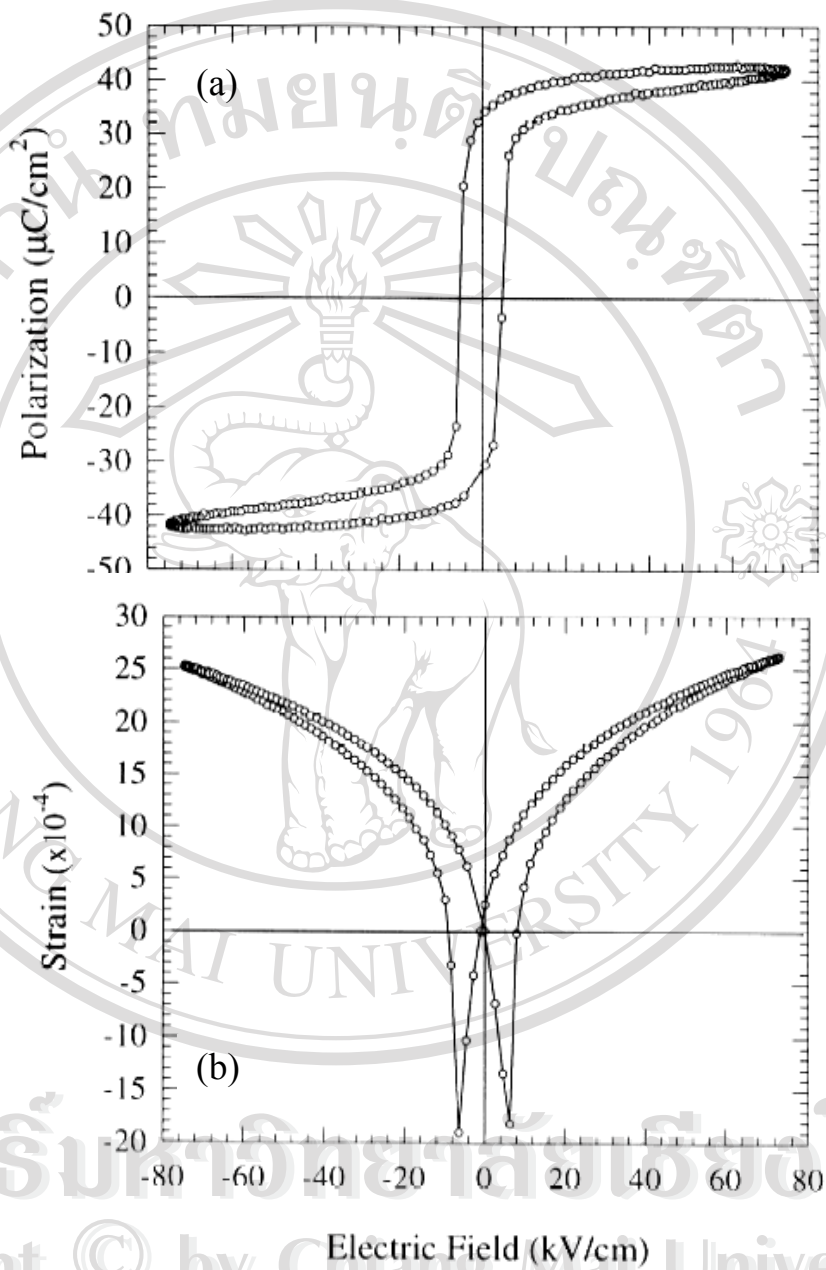


Figure 1.12 (a) Room temperature dielectric hysteresis loops for PNNZT ceramics
(b) Room temperature field induced strain for PNNZT ceramics.⁴⁵

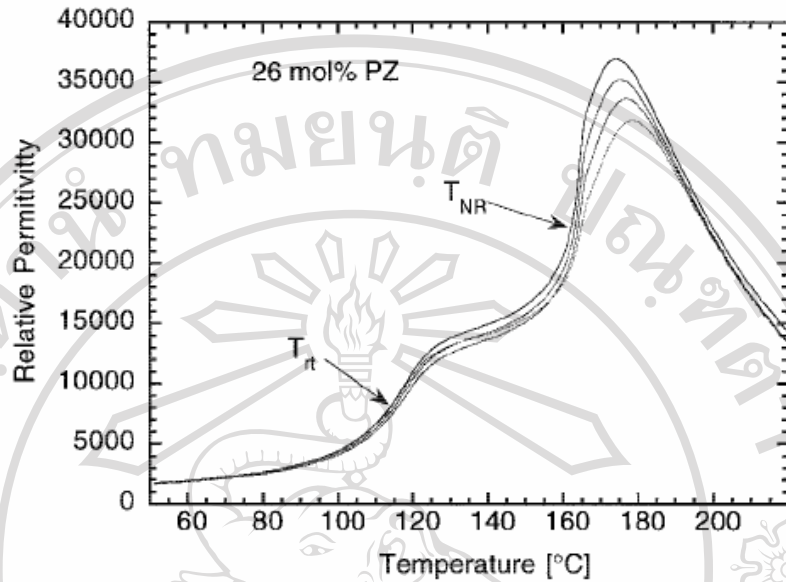


Figure 1.13 Permittivity versus temperature curves for the 26 mol% PZ composition.⁴⁶

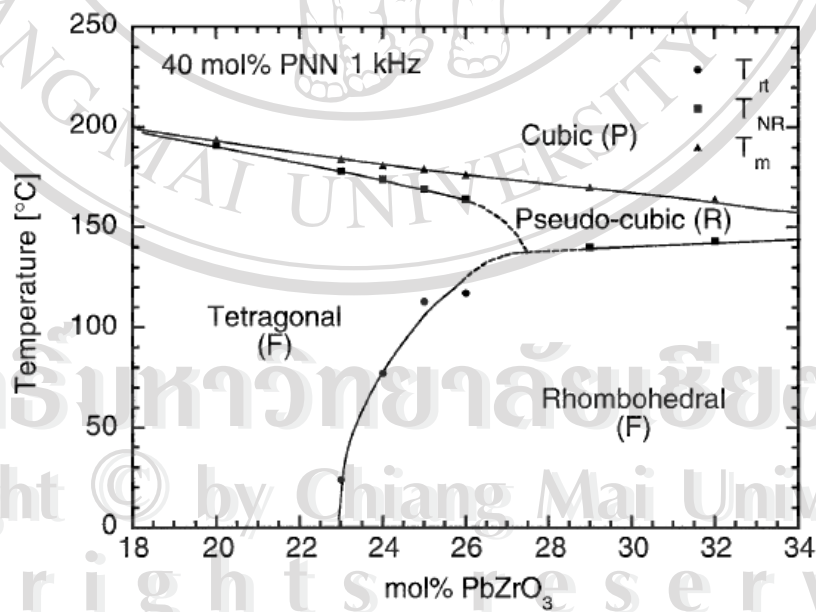


Figure 1.14 Proposed phase diagram for a PNN–PZT system containing 40 mol% PNN, measured at 1 kHz (“F” denotes normal ferroelectric, “R” denotes relaxor ferroelectric, and “P” denotes paraelectric).⁴⁶

The $0.4\text{Pb}(\text{Ni}_{1/3},\text{Nb}_{2/3})\text{O}_3 - x\text{PbZrO}_3 - (0.6-x)\text{PbTiO}_3$ ($0.2 < x < 0.32$)(40PNN–60PZT) compositions were selected for this work. This material exhibits an MPB that curves towards the zirconium rich region and a spontaneous transition from normal to relaxor ferroelectric behavior for all the compositions tested. The results showed that the temperature at which the 1 kHz permittivity is maximum (hereafter denoted as T_m) decreased linearly as the molar fraction of PZ increased. In addition to the principal peak, two types of anomalies could be observed and they are marked on Fig. 1.13 for the 26 mol% PZ composition.

This phase diagram pattern (Fig. 1.14) is suggested as applicable to other relaxor – ferroelectric systems and especially to the PZN–PT and PMN–PT systems. This would provide a new interpretation for the region of sharp MPB bending in terms of the appearance, at high temperatures, of a relaxor phase rather than a ferroelectric tetragonal phase.